

Development of a combined radiation and full thickness burn injury minipig model to study the effects of uncultured adipose-derived regenerative cell therapy in wound healing

Philippe Foubert, Melanie Doyle-Eisele, Andreina Gonzalez, Felipe Berard, Waylon Weber, Diana Zafra, Zeni Alfonso, Sherry Zhao, Mayer Tenenhaus & John K. Fraser

To cite this article: Philippe Foubert, Melanie Doyle-Eisele, Andreina Gonzalez, Felipe Berard, Waylon Weber, Diana Zafra, Zeni Alfonso, Sherry Zhao, Mayer Tenenhaus & John K. Fraser (2016): Development of a combined radiation and full thickness burn injury minipig model to study the effects of uncultured adipose-derived regenerative cell therapy in wound healing, International Journal of Radiation Biology, DOI: [10.1080/09553002.2017.1242814](https://doi.org/10.1080/09553002.2017.1242814)

To link to this article: <http://dx.doi.org/10.1080/09553002.2017.1242814>

 View supplementary material 

 Accepted author version posted online: 03 Oct 2016.
Published online: 21 Oct 2016.

 Submit your article to this journal 

 Article views: 17

 View related articles 

 View Crossmark data 

RESEARCH ARTICLE

Development of a combined radiation and full thickness burn injury minipig model to study the effects of uncultured adipose-derived regenerative cell therapy in wound healing

Philippe Foubert^a, Melanie Doyle-Eisele^b, Andreina Gonzalez^a, Felipe Berard^b, Waylon Weber^b, Diana Zafra^a, Zeni Alfonso^a, Sherry Zhao^a, Mayer Tenenhaus^c and John K. Fraser^a

^aCytori Therapeutics Inc, San Diego, CA, USA; ^bLovelace Respiratory Research Institute, Albuquerque, NM, USA; ^cUCSD Medical Center, University of California, San Diego, CA, USA

ABSTRACT

Purpose: To develop an approach that models the cutaneous healing that occurs in a patient with full thickness thermal burn injury complicated by total body radiation exposure sufficient to induce sub-lethal prodromal symptoms. An assessment of the effects of an autologous cell therapy on wound healing on thermal burn injury with concomitant radiation exposure was used to validate the utility of the model.

Methods: Göttingen minipigs were subjected to a 1.2Gy total body irradiation by exposure to a 6 MV X-ray linear accelerator followed by $\sim 10\text{cm}^2$ full thickness burns (pre-heated brass block with calibrated spring). Three days after injury, wounds were excised to the underlying fascia and each animal was randomized to receive treatment with autologous adipose-derived regenerative cells (ADRC) delivered by local or intravenous injection, or vehicle control. Blood counts were used to assess radiation-induced marrow suppression. All animals were followed using digital imaging to assess wound healing. Full-thickness biopsies were obtained at 7, 14, 21 and 30 days' post-treatment.

Results: Compared to animals receiving burn injury alone, significant transient neutropenia and thrombocytopenia were observed in irradiated subjects with average neutrophil nadir of $0.79 \times 10^3/\mu\text{l}$ (day 15) and platelet nadir of $60 \times 10^3/\mu\text{l}$ (day 12). Wound closure through a combination of contraction and epithelialization from the wound edges occurred over a period of approximately 28 days' post excision and treatment. Re-epithelialization was accelerated in wounds treated with ADRC (mean 3.5-fold increase at 2 weeks post-treatment relative to control). This acceleration was accompanied by an average 67% increase in blood vessel density and 30% increase in matrix (collagen) deposition. Similar results were observed when ADRC were injected either directly into the wound or by intravenous administration.

Conclusions: Although preliminary, this study provides a reproducible minipig model of thermal burn injury complicated by myelosuppressive total body irradiation that utilizes standardized procedures to evaluate novel countermeasures for potential use following attack by an improvised nuclear device.

ARTICLE HISTORY

Received 8 February 2016
Revised 11 July 2016
Accepted 20 September 2016

KEYWORDS

Adipose-derived regenerative cells; combined injuries; radiation; thermal burn

Introduction

The Government Accountability Office of the United States Government has estimated that, in the event of an attack with an improvised nuclear device (IND), as many as 10,000 persons could receive flash, flame and/or contact burns that are complicated by exposure to radiation (United States Government Accountability Office 2012). Injuries of this type were evident in 60–70% of the immediate survivors of the detonations over Hiroshima and Nagasaki in 1945 (Iijima 1982) and following the reactor meltdown at Chernobyl in 1986 (Barabanova 2006). As a result of plausible threats from nuclear attack or accident, the development of animal models for bio-defense research and for evaluation of novel countermeasures has been initiated (Williams et al. 2010).

Efforts to identify and establish a representative model generally requires a review of current literature, appropriate

physiologic data and end points, as well as established precedent. The Göttingen minipig has been well studied for the evaluation of the effects of acute radiation. A number of investigators have utilized the porcine model to evaluate hematopoietic recovery following total body irradiation (Pennington et al. 1988; Colby et al. 2000; Moroni et al. 2013). While rat, mouse, and rabbit models have been used in experimental and toxicological dermatologic studies, porcine skin is generally considered to be more representative of human skin than these small animals (Sullivan et al. 2001). A number of porcine thermal burn models have often been advocated for evaluating wound healing and novel treatments (Singer and McClain 2003; Cuttle et al. 2006; Branski et al. 2008). While the treatment of wounds following total-body irradiation has been evaluated in mouse models (Palmer et al. 2011; Kiang et al. 2014), there is no

well-established large animal model evaluating burn wound healing in the context of total-body irradiation. The primary purpose of this study was to address this deficiency by developing a minipig model that mimics the clinical profile of a patient with thermal burn injuries triaged to receive treatment following a mass casualty event involving detonation of an improvised nuclear device. This was achieved by selecting a radiation dose that led to substantial, but sub-lethal, marrow suppression combined with a modest sized full thickness thermal burn injury. Patients with a higher level of radiation exposure and/or considerably larger burns would be at a substantially higher risk of mortality and a correspondingly lower likelihood of being triaged to receive treatment.

A mass casualty event involving a large number of burn casualties is expected to severely stress available burn care resources, particularly the availability of highly experienced burn care surgeons and nursing staff skilled in the care of acute burn patients and the application of autologous skin grafts, skin substitutes, xeno- and allo-grafts far beyond capacity. As a result, there is increasing interest in developing new regenerative medicine strategies for casualty burn care. Cell-based therapy represents a promising strategy to induce tissue repair and regeneration in normal and irradiated subjects (Forcheron et al. 2012; Riccobono et al. 2012; Gardien et al. 2014). Specifically, advances in the understanding of adipose tissue Stromal Vascular Fraction (SVF) cells as a candidate cell therapy to promote wound healing (Akita et al. 2012; Huang et al. 2013; Atalay et al. 2014; Kokai et al. 2014). We refer clinical grade SVF cells as adipose-derived regenerative cells (ADRC) (Fraser et al. 2014). In an effort to better understand their potential, we evaluated safety and tolerability of local as well as intravenously administered autologous ADRC and assessed, in preliminary fashion, their effects on wound healing using a novel model of concomitant radiation and thermal burn injury.

Materials and methods

Animals

This study was conducted in accordance with applicable federal and state guidelines, and was approved by the Institutional Animal Care and Use Committee of the Lovelace Biomedical and Environmental Research Institute (LBERI). Fourteen male Göttingen minipigs (6–8 months; 9–16 kg) were received from Marshall BioResources (North Rose, NY) and were quarantined for 14 days prior to study assignment by body weight stratification using a computerized data acquisition system (Provantis[®] 8.2). Animals were identified by ear tags, cage cards and/or color identifiers on the animal's back.

Total body irradiation and dosimetry

For the irradiation procedure, animals were sedated with 1.1 mg/kg acepromazine (IM) and transported to the irradiation room within the LINAC (Linear Accelerator) facility. The animals were fully anesthetized with isoflurane (5% for

induction, 1–3% for maintenance) via face mask. Isoflurane anesthesia was utilized during the entire irradiation and thermal burn procedures. Once the animals were anesthetized, they were carefully supported and wrapped in a bolus tissue-equivalent material ('SuperFlab') and ventrally placed in a sling restraint with their legs carefully tucked under their bodies. The animals were adjusted to ensure they were entirely positioned inside of the irradiation field. The physical dimensions of each animal were measured and entered into a validated Excel spreadsheet to determine the LINAC settings necessary to achieve a total body irradiation dose of 1.2 Gy delivered to the midline of the animal using the LBERI Varian 600c LINAC. Animals were positioned with their left lateral surface facing the LINAC beam, administered 0.6 Gy to the midline, rotated 180 degrees such that the right lateral surface was facing the LINAC beam, and administered another 0.6 Gy to the midline of the animal. The target dose rate to the midline of the animal was 0.6 Gy/min. The dose was measured by placement of solid state diode detectors (P/N: 11630000-2, Sun Nuclear Corp, Melbourne, FL) on the hips and shoulders. The delivered midline dose was determined by summation of the entrance and exit doses. The LINAC was calibrated in accordance with the American Association of Physics in Medicine (AAPM) Task Group Report 106. The LINAC output was verified daily against a NIST traceable PTW ion chamber (TN30013-005353, CNMC Company, Nashville, TN). The diode measurements were also verified daily prior to irradiation procedures.

Full thickness thermal burn injury

Following the irradiation procedure, a full thickness thermal burn was applied under the same anesthetic event as the irradiation procedure. The dorsum of each anesthetized animal was clipped and surgically scrubbed, prepped and draped. Six full thickness burns were induced on the dorsum of each animal; three on left side (designated L1, L2, and L3; cranial to caudal) and three on the right side (similarly designated R1, R2, and R3). Wounds were created by applying a custom-made device comprising a pre-heated brass block (3.5 cm diameter; 350 g; heated to 180–200 °C) and a calibrated spring-based housing that applied the heated block at a pressure of 0.4 kg/cm² for 1 min. The temperature of the block was verified using a laser thermometer immediately prior to each application. The burn procedure was previously validated to induce a reproducible full thickness thermal burn in the Göttingen strain of pig (Foubert et al. 2015). Burns (~10 cm² each) were uniformly created 3.5 cm apart from each other and 4 cm away from the midline of the dorsum. Reproducible and symmetric positioning was facilitated by the use of a custom-made stencil template and markings prior to injury. Following induction of the thermal injury, burn wound sites were treated by topical application of a triple antibiotic cream (Water-Jel Technologies, Carlstadt, NJ) and covered with non-adherent bandage pads (Telfa bandage), secured with Ioban (3M Corporation, St. Paul, MN), elastic wraps and a Lomir jacket. Minipigs were allowed to

fully recover from anesthesia in their transfer cage and then returned to their home cages post recovery.

For pain management, animals had a fentanyl patch (25 µg) placed behind the ear on Day -1. The patch was changed every other day through Day 12, at which point the study veterinarian determined that the patches could be safely removed. No special hematopoietic supportive care (e.g. hematopoietic growth factor support such as filgrastim) was provided.

Adipose-derived regenerative cells (ADRC) isolation

Three days after radiation and burn injury (prior to excision of burn wounds), animals were anesthetized with an intramuscular injection of 10 mg/kg ketamine with 2 mg/kg xylazine. Anesthesia was maintained with inhalation of 3–5% isoflurane. Adipose tissue (9–25 g) was excised from the inguinal fat pad, minced, and then digested with Celase[®] enzyme (1 U/ml) as previously described (Foubert et al. 2015). ADRC yield and viability were measured automatically using the cell counting device NucleoCounter[®] NC-100[™] (ChemoMetec, Denmark).

Wound excision and treatment

Three days post-injury, the full thickness eschar was excised to the level of the underlying muscular fascia using sterile technique as previously described (Foubert et al. 2015). Immediately following wound excision, animals were randomized to receive control Lactated Ringer's (LR) ($n=4$), intravenous ($n=6$) or local sub-dermal/sub-fascial injections ($n=4$) of freshly isolated ADRC. Wounds treated with local delivery received 0.25×10^6 ADRC $\pm 25\%$ per cm^2 injected sub-dermally and into the superficial fascia (total of 25 injections of 0.2 ml per wound site; average of $19.5 \times 10^6 \pm 4 \times 10^6$ ADRC per animal). Animals randomized to the intravenous ADRC arm were treated with a 5 ml infusion delivered through the ear vein at a rate of 1 ml/min at an average cell dose of 1.5×10^6 ADRC/kg of body weight (average of $21 \times 10^6 \pm 6.8 \times 10^6$ ADRC per animal). Control groups received treatment with vehicle (LR) alone.

To protect the wounds from outside contamination and infection, a multi-layer dressing was used. The first dressing layer, placed onto the wound site consisted of silver-impregnated soft foam dressing (Mepilex[®]-Ag; Molnlycke health Care AB, Goteborg, Sweden). A second dressing layer of loba[™] (antimicrobial incise drape with an iodophor impregnated adhesive) was applied over the Mepilex to seal off the wound fields. The third layer of coverage consisted of a cotton elastic bandage wrap. Finally, a Lomir jacket was placed to secure the dressings. Dressings were changed every 5–7 days in order to minimize infection throughout the course of the study.

Characterization of porcine ADRC

Tissue samples from animals randomized to the control LR group (not treated with ADRC) were transported overnight to

Cytori Therapeutics, processed and stained with CD45-FITC (clone K252.1E4; Serotec), CD31-PE (clone LCI-4; Serotec), CD90-PerCP-Cy[™]5.5 (clone 5E10; BD Biosciences) and CD146-PE (P1H12; BD Biosciences), as previously described (Foubert et al. 2015). Acquisition and analysis of the cells were performed on FACSaria using FACSDiva software.

Clonogenic assay (CFU-F)

Isolated porcine ADRC were plated in six-well plates at low density (100 cells/ cm^2) in DMEM/F12 containing 10% Fetal Bovine Serum (FBS). After 12–14 days, cells were rinsed with PBS, fixed with formalin, and stained with Hematoxylin solution (Hemacolor kit; EMD Millipore). Colonies containing >50 colony-forming unit fibroblasts (CFU-F) were counted. CFU-F frequency was calculated by dividing the number of colonies by the number of seeded cells.

Endothelial tube formation in vitro assay

The presence of functional endothelial cells was evaluated using a tube formation assay (Foubert et al. 2015). This assay measures the ability of endothelial cells, given the appropriate time and extracellular matrix support, to migrate and form capillary-like structures in vitro. Briefly, isolated ADRC were plated at a density of 12,500 cells per cm^2 (i.e. 25,000 cells in 3 ml of media) in a 24-well plate. Cells were cultured in Endothelial Growth Media (EGM-2, Lonza) which was changed every 3 days. After 2 weeks, cells were fixed and stained with CD31 antibody (Clone JC07A, Dako). Endothelial branching was digitally quantified using the Angio Tool software (<https://ccrod.cancer.gov/confluence/display/ROB2/Home>).

In vitro adipogenesis assay

Differentiation towards adipocytes is one of the hallmarks of adipose stem and progenitor cells. ADRC were cultured for 2 weeks in adipogenic medium (Adipocyte Differentiation Medium; ZenBio). The presence of adipocytes was assessed by Oil-Red-O staining.

Planimetry wound imaging

Digital imaging of wounds was conducted on day 0 (post-burn), day 3 (pre- and post-excision), days 10, 17, 23 and 33 post-injury (i.e. days 7, 14, 21 and 30 post-treatment). Digital images were captured using the SilhouetteStar[™] Wound Camera (ARANZ Medical, Christchurch, New Zealand). Wound images were then reviewed and the total wound area was measured using the Silhouette Connect[™] System (ARANZ Medical, Christchurch, New Zealand).

Wound histology

Histologic assessment was performed on 6 mm biopsies collected at the leading edge of re-epithelialization and from the center of the wound on days 10, 17, 23 and

21 post-injury. Biopsies were fixed in 10% Neutral-Buffered Formalin (NBF), embedded in paraffin, sectioned (5 μm), and stained with hematoxylin and Eosin (H&E) and Masson Trichrome stain. Entire slides were then digitally scanned using the Aperio ScanScope AT2 slide scanner (Aperio Technologies). Slides were viewed and analyzed using the ImageScope viewer. The ImageScope analysis software package (version 12.1; Aperio Technologies) was applied to quantify histochemical staining.

Immunohistochemistry

Tissue specimens were fixed in 10% normal buffered formalin and subsequently embedded in paraffin. Paraffin-embedded tissue sections (5 μm) were deparaffinized and re-hydrated through alcohol to water. Sections were next incubated with BLOXALL Solution (Vector Laboratories) for 10 min to inactivate endogenous peroxidase activity. Tissue sections were subsequently subjected to an antigen retrieval step by boiling sodium citrate solution (pH 6, Vector Laboratories) for 15 min in a pressure cooker. An anti-CD31 antibody (5 $\mu\text{g}/\text{ml}$, Abbiotec) was used for immunodetection of blood vessels on paraffin-embedded skin sections. Peroxidase-based detection of the primary antibody was performed using a Vectastain Elite ABC kit (Vector Laboratories) according to the manufacturer's instructions, followed by 3, 3'-diaminobenzidine (DAB) incubation and nuclear staining with hematoxylin. As controls, tissue sections were treated as described above without adding primary antibody. CD31 was quantified on two slides per wound assessing the entire section on each slide using whole slide ImageScope analysis software (Microvessel Analysis Algorithm; Aperio Technologies). The number of vessels per surface area was calculated using the micro-vessel analysis algorithm (Aperio Technologies).

Digital quantification of collagen deposition

The Deconvolution Analysis algorithm (Aperio Technologies) was used to quantify Masson's trichrome staining as previously described (Foubert et al. 2015). As with CD31 staining, two slides per wound were assessed across the entire section on each slide. The software algorithm makes use of a deconvolution method to separate different colors, so that quantification of individual stain is possible without cross contamination. This algorithm calculates the percentage of weak (1+), medium (2+), and strong (3+) collagen positive staining. Employing this technique, a collagen deposition score was calculated by a simple formula involving the positive percentages (Score = $1 \times [\% \text{Weak}] + 2 \times [\% \text{Medium}] + 3 \times [\% \text{Strong}]$).

Peripheral blood counts

Myelosuppression was monitored by regular blood cell counts. Prior to blood collection all animals were sedated with acepromazine (of 0.5–1.1 mg/kg, IM). Blood was collected via the saphenous vein and placed into vacutainers containing potassium-EDTA as anticoagulant. Blood draws

were performed 5 days before irradiation injury, and on days 0, 3, 5, 8, 10, 12, 15, 20, 23, 25, 30 and 33 post-irradiation. Samples were analyzed by automated analysis using an ADVIATM 120 Hematology System (Bayer Corporation). Samples that exhibited any evidence of clotting were excluded from the analysis.

Cytokine quantitation by ELISA

Concentration of IL-6 (DuoSet[®], R&D Systems) and C-reactive protein (CRP) (Innovative Research) in blood serum were assessed using commercially available porcine-specific Enzyme-linked immune sorbent assay (ELISA) kits according to the manufacturer's instructions. Samples were measured using a plate reader (SpectraMax, Molecular Devices) set at an absorbance of 450 nm.

Statistical analysis

Results are expressed as means \pm SEM. Comparisons between two groups were performed using an unpaired *t*-test (Graph Pad Prism version 6.07). A one-way ANOVA was used to compare the means of more than two independent groups. A value of $p < .05$ was considered significant.

Results

Total body irradiation and hematological changes

Using the methodology previously described, the measured midline doses to the animals during irradiation resulted in an average absorbed dose of 1.23 ± 0.04 Gy. The measured dose rate to the midline of the animal ranged from 0.48–0.57 Gy/min. The sub-lethal nature of this dose was demonstrated by the observation that no animals died during the study despite absence of supportive measures beyond simple wound care.

Complete blood counts were performed to assess the combined effects of radiation and burn injury on hematopoietic parameters (Figure 1). This 1.2-Gy radiation dose consistently induced significant, rapid leukopenia and thrombocytopenia (Figure 1). Compared to animals subjected to burn injury alone, White blood cell (WBC) counts exhibited a progressive decline over the first 24 days followed by a partial recovery in combined radiation and burn injury animals (Figure 1(a)). This decline was led by a 60% decline in lymphocyte count over the first 3 days' post-injury (Figure 1(b)). In the combined injury group, neutrophil counts were generally stable through days 8–10 before dropping precipitously to a nadir at day 15 ($<1000/\mu\text{l}$) (68% reduction). Neutrophil counts remained below baseline throughout the remainder of the study (day 30 post-irradiation) (Figure 1(c)). Platelet counts in all animals remained generally stable through Day 5 post-injury. Animals subjected to radiation and burn injury exhibited a nadir in platelet count of approximately $100,000/\mu\text{l}$ or lower between days 10 and 15 after radiation exposure (average 86% reduction) (Figure 1(d)). Combined-injured, animals generally exhibited a slow

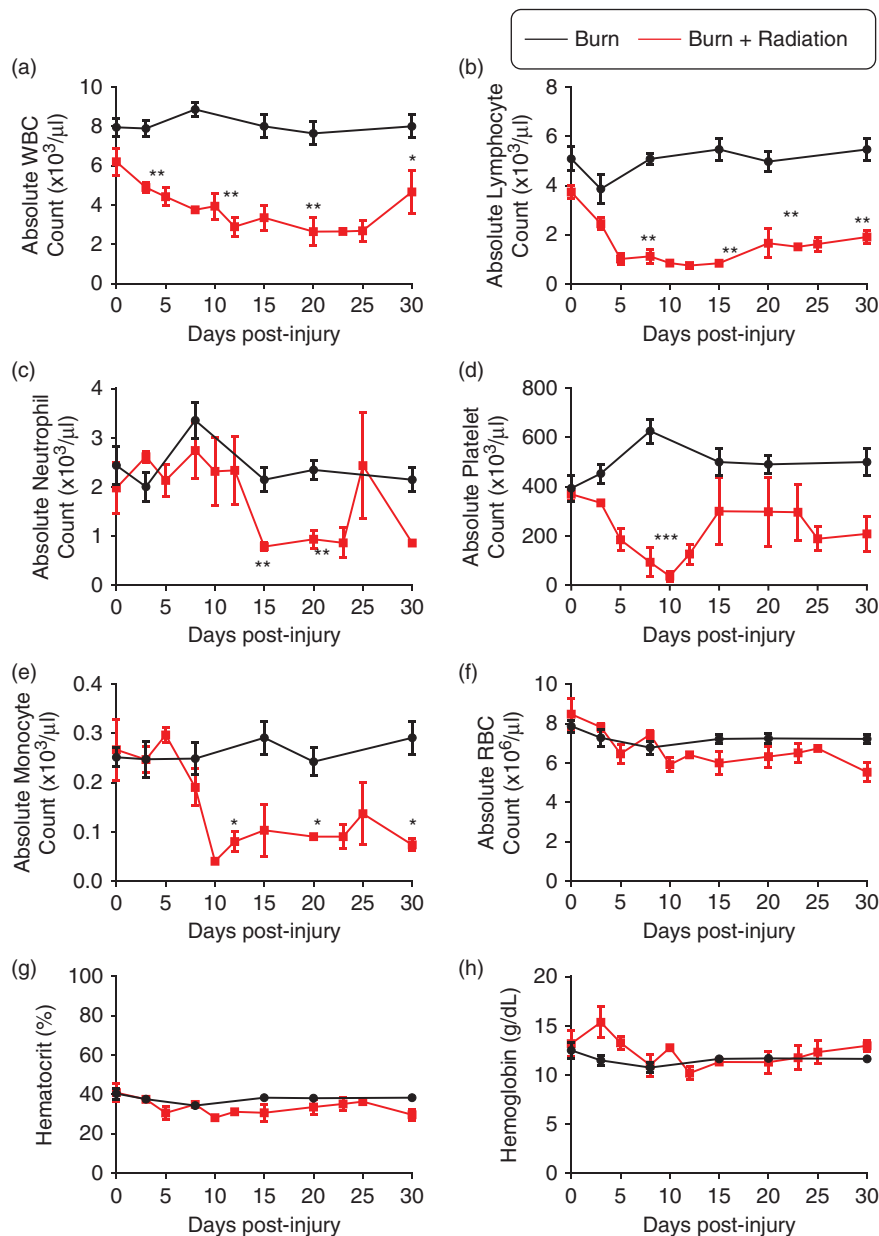


Figure 1. Evaluation of hematological parameters after burn injury alone and combined injury (radiation and burn). Animals were exposed to total body irradiation with a single 1.2 Gy dose of X-rays using a linear accelerator (LINAC) at 0.6 Gy/min. Blood cell loss and recovery were evaluated. (a) White blood cells, (b) lymphocytes, (c) neutrophils, (d) platelets, (e) monocytes, (f) Red blood cells, (g) hematocrite and (h) hemoglobin. $n = 4/\text{group}$; Results are presented as mean \pm standard error of mean (SEM). * $p < .05$; ** $p < .01$; *** $p < .001$ versus burn injury alone ($n = 4$ animals per group).

return toward normal platelet levels after 15 days. Monocytes were also affected by the radiation injury with a nadir of about $30/\mu\text{l}$ observed at day 10 post-injury (Figure 1(e)). Finally, red blood cell (RBC) count, hematocrit and hemoglobin levels declined by approximately 20% over baseline following radiation exposure (Figure 1(f, g)).

Altogether, these data demonstrated that a radiation dose of 1.2 Gy leads to substantial sub-lethal hematologic injury in Göttingen minipigs subjected to burn injury.

Effects of combined injury on the systemic inflammatory response

To further elucidate the effects of combined injury on systemic inflammation, we measured key pro-inflammatory

cytokines (IL-6 and CRP) in the circulating blood of animals subjected to burn only or combined radiation and burn injury (Supplementary Figure 1, available online). Circulating IL-6 was not detectable in both groups at baseline and at any time-point post-injury (data not shown). In contrast, CRP levels were altered in both groups at 7 and 14 days' post-injury. In burn-only animals, CRP levels peaked at day 7 post-injury ($372.9 \pm 27.3 \mu\text{g/ml}$) and returned to baseline level by day 14 post-injury. Importantly, at 7 and 14 days' post-injury, CRP levels were significantly increased in combined injured-animals compared to burn animals only (4.3- and 2.9-fold, respectively; $p < .001$). This data confirmed that radiation injury induces increased production of CRP in our large animal model and are consistent with published data in non-human primates (Valente et al. 2015) and mice (Kiang and Ledney 2013).

Full thickness thermal burn injury

The custom-made burn induction device created reproducible, full thickness wounds as assessed by both gross observation (Figures 2(a) and (b)) and histologic assessment of excised material. Histologically, total disruption of the dermal epithelium and extensive damage of the entire dermis with collagen denaturation through the sub-cutaneous adipose tissue was observed. Loss of viable tissue was observed as color change from blue (healthy connective tissue) to red (coagulated tissue) (Figure 2(c)). This feature, which is hallmark characteristics of full thickness burn injury, was observed in all wounds assessed at the time of excision of the injured skin demonstrating consistent, reproducible full thickness burn injury.

ADRC isolation and characterization from irradiated animals subjected to burn injury

ADRC were successfully isolated from the inguinal fat pads of irradiated animals on day 3 post-injury. Cell yield ($1.6 \pm 0.2 \times 10^6$ viable nucleated cells/g of tissue processed) and viability ($90.4 \pm 4.5\%$) were similar to those we have

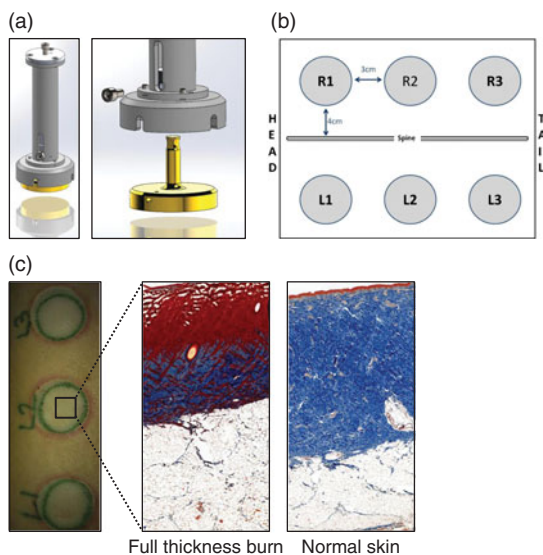


Figure 2. Induction of full thickness burn injury using a custom-made template and device. (a) Full thickness burns were created by applying a pre-heated brass block (10 cm^2 ; 350 g; heated to $180\text{--}200^\circ\text{C}$) at a pressure of 0.4 kg/cm^2 to the dorsum of the animal for 1 min, using a custom-built, calibrated device. (b) A printed wound template sheet was designed to ensure that the six dorsal wound sites (three along each side of the spine) were uniformly 3 cm apart and located 4 cm from the spine of the minipig. From cranial to caudal, the wound sites were labeled L1, L2, and L3 for wounds on the left side and R1, R2, R3 for wounds on the right side. (c) Representative images of burn wounds, dermal tissue 72 h after burn injury and healthy skin stained with Masson's Trichrome.

previously observed with non-irradiated animals (Table 1) (Foubert et al. 2015). Flow cytometric assessment of the ADRC indicated the presence of leukocytes (CD45^+ cells; $19.8 \pm 5\%$), endothelial cells ($\text{CD31}^+/\text{CD45}^-$ cells; $9.6 \pm 3\%$), stromal cells (fibroblast and fibroblast-like; $\text{CD90}^+/\text{CD45}^-$ cells; $42.5 \pm 6.35\%$) and smooth muscle-related cells (SMC; $\text{CD31}^-/\text{CD146}^+/\text{CD45}^-$ cells; $22.4 \pm 6.2\%$) (Figure 3(a)). These numbers and proportions are similar to those previously reported for non-irradiated animals (Figure 3(a)) (Foubert et al. 2015). Content of fibroblast-like cell colony forming units (CFU-F; $4.0 \pm 0.8\%$) was also similar to that seen in non-irradiated animals (Figure 3(b)) (Foubert et al. 2015). ADRC from animals subjected to either burn injury alone or combined radiation and burn injury also exhibited the capacity to form vessel-like tubes comprised of CD31^+ endothelial cells (Figure 3(c)) as well as the capacity to differentiate into adipocytes under appropriate culture conditions (Figure 3(d)), without any apparent difference noted between both groups (data not shown).

Safety of local and intravenous ADRC treatment

This model was then used to assess the safety and efficacy profile of ADRC therapy for thermal burn injury complicated by concomitant radiation exposure. For this purpose, animals were randomized to receive either locally injected control LR ($n = 4$ animals, 24 wounds each), locally injected ADRC ($n = 4$ animals, 24 wounds each) or intravenously administered ADRC ($n = 6$ animals, 36 wounds). All subjects enrolled survived the 30-day study period. Local and intravenous ADRC delivery were well tolerated and no serious side-effects related to body weight, loss of appetite, infection, activity, or complete blood counts was observed over the course of the study (data not shown). As shown in Supplementary Figure 2, ADRC administration (via local or intravenous [iv] delivery) did not modulate any of the measured hematopoietic parameters.

Efficacy of local and intravenous ADRC treatment on burn wound healing in irradiated animals

Effects on wound re-epithelialization

Re-epithelialized wound area was visually identified as a glistering reflecting pink/purple fragile dry thin layer region whereas granulating open areas were identified as having a vascular berry-like red and most moist appearance (Figure 4(a)). No epithelialization was evident by planimetry at day 7-post treatment in any group. Planimetric analysis revealed that wound epithelialization at day 14 post-treatment was increased by 25% compared with control in the local ADRC arm and by 36% in the intravenous delivery arm

Table 1. Adipose tissue harvest and adipose-derived regenerative cells (ADRC) isolation characteristic in animals subjected to combined injury (radiation + burn).

Radiation + burn injury	Age (months)	Body weight (kg)	Viable ADRC yield ($\times 10^6/\text{g}$ of tissue)	ADRC viability (%)	Total viable cells administered ($\times 10^6$)
Control ($n = 4$)	7.3 ± 0.5	12.6 ± 2.4	1.8 ± 1.1	86.8 ± 5.1	n/a
Local ADRC ($n = 4$)	7.4 ± 0.4	13.3 ± 0.9	1.6 ± 0.5	93.9 ± 4.2	19.5 ± 8
Iv ADRC ($n = 6$)	7.0 ± 0.7	12.7 ± 1	1.5 ± 0.4	90.2 ± 4.8	20.9 ± 6.6

Data are presented as mean \pm standard deviation.

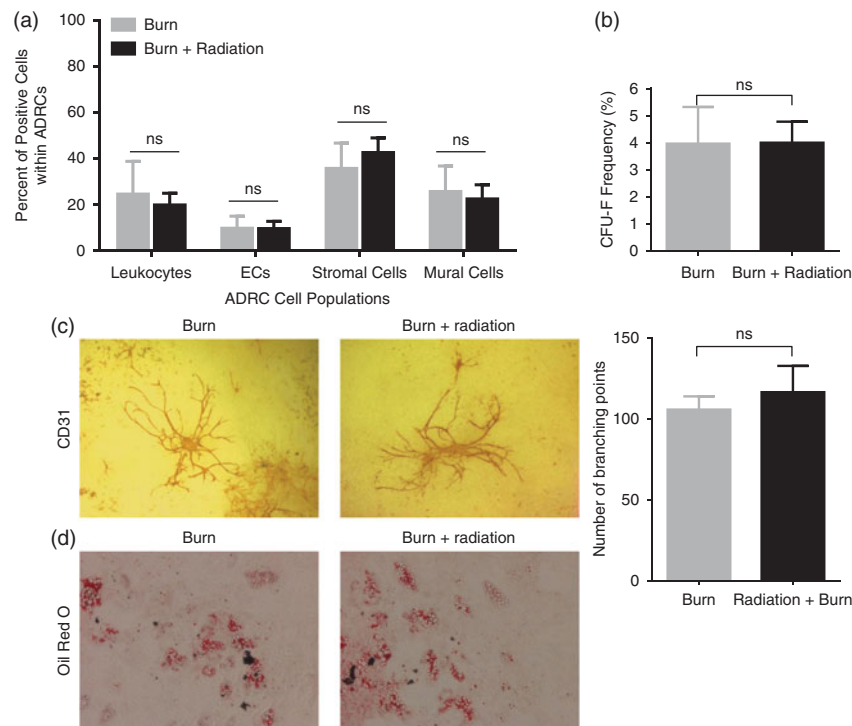


Figure 3. Isolation of viable and functional ADRC from burn injury alone and combined injured (radiation and burn) minipigs. (a) Porcine ADRC characterization in animals subjected to burn injury alone and combined injury. The presence of leukocytes, endothelial cells (EC), stromal cells and mural cells was analyzed using CD45, CD31, CD90 and CD146 cell surface markers. (b) The fibroblastoid colony-forming unit (CFU-F) assay was performed to define the number of progenitor cells in animals subjected to burn injury alone and combined injury. (c) Differential potential of ADRC towards endothelial cell. ADRC cells were cultured in EGM-2 media. Endothelial cell differentiation into capillary-like structures was quantified by immunostaining for CD31 on day 14. (d) Differential potential of ADRC towards adipocyte lineage. ADRC cells were cultured in DMEM/F12 with 10% FCS. Presence of mature adipocytes was measured by Oil Red O stain on day 14. $n = 4$ burn injury alone and $n = 4$ combined injury (radiation + burn). ns: non-significant.

($78\% \pm 4.7\%$ vs. $85.6\% \pm 3.1\%$ vs. $62.3\% \pm 6.7\%$, respectively; $p < .05$ for comparison to control for each delivery route). There was no significant difference noted on planimetry between the two delivery routes (Figure 4(a)). By day 23, all wounds were completely epithelialized. Wound re-epithelialization was confirmed by histological assessments using H&E staining. On day 14 post-treatment, epithelial coverage increased over control by 3.5- and 2.5-fold after local and intravenous ADRC treatment, respectively ($25.5\% \pm 10.6\%$ vs. $23.4\% \pm 8.6\%$ vs. $7.9\% \pm 2.9\%$, respectively; $p < .05$ for comparison to control for each delivery route) (Figure 4(b)). Biopsies on days 21 and 30 showed complete re-epithelialization for all treatment groups (Supplementary Figure 3).

Effects on wound vascularization

To determine the kinetics of neovascularization within the wound tissue, immunohistochemical analysis was performed on biopsies collected at days 7, 14 and 21 post-treatment. For all groups, the number of CD31-positive blood vessels peaked at days 7–14 then decreased by day 21 post-treatment. At day 7, microvessel density (MVD) showed a 45% and 48% increase in local and intravenously ADRC-treated wounds compared to those treated with control LR, respectively (72 ± 10.6 vs. 74.3 ± 16.2 vs. 49.8 ± 13.4 vessels per mm^2 , respectively; $p = .05$ for each comparison; Figure 5). At day 14, MVD was 67% and 45% greater in animals receiving local and intravenous ADRC compared to LR control, respectively (80.7 ± 13.8 vs. 69.5 ± 8.6 vs. 48.2 ± 7.08 vessels per mm^2 ,

respectively; $p = .04$ and $p = .06$; Figure 5). No significant difference was observed between groups at day 21 post-treatment.

Effects on collagen deposition

Digital quantification of collagen deposition in wound biopsies collected at day 30 post-treatment showed a trend towards increased collagen deposition by 29% in wounds treated with local ADRC injection compared to control LR treatment (Collagen score: 81.1 ± 6.3 vs. 61.8 ± 6.6 , respectively; $p = .06$). Intravenous administration of ADRC did not appear to modulate collagen deposition at day 30 post-treatment (Figure 6).

Discussion

The successful development of novel medical countermeasures against nuclear threats requires the development of well-characterized animal models which clinically reflect anticipated combination injury patterns as well as physiologic effects. The Göttingen minipig is a suitable model for studies of Acute Radiation Syndrome (ARS) and for cutaneous injury. Although the $\text{LD}_{50/30}$ in these animals is lower than that for humans, radiation-induced hematological changes are very similar (Moroni et al. 2013). The minipig model presented herein comprises radiation exposure sufficient to damage the bone marrow combined with full thickness burn injury. To our knowledge, this is the first reported large animal model

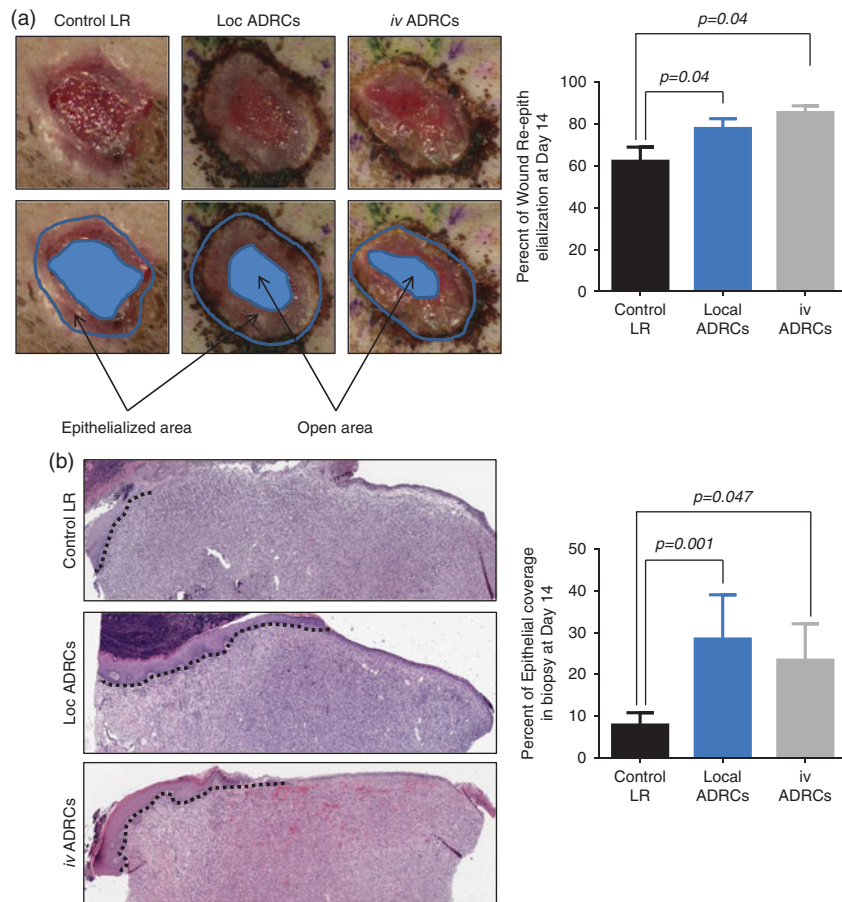


Figure 4. Effect of ADRC on wound re-epithelialization after concomitant radiation and burn injury. (a) Digital images of wound showing wound epithelialization at day 14 post-treatment. Entire wound size and open wound area were manually traced and measured by planimetry using computer software to determine the mean percent of wound epithelialization on day 14. (b) Representative photomicrographs of sections stained with Hematoxylin Eosin (H&E) and quantification of wound re-epithelialization. Dotted lines delineate the neo-epithelium from the dermal tissue. The percent of re-epithelialization was calculated by measuring the length of neo-epidermis in cross-section and dividing it by the specimen's diameter. $n = 4-6$ animals/group ($n = 18-25$ wounds per group). Results are presented as mean \pm standard error of mean (SEM).

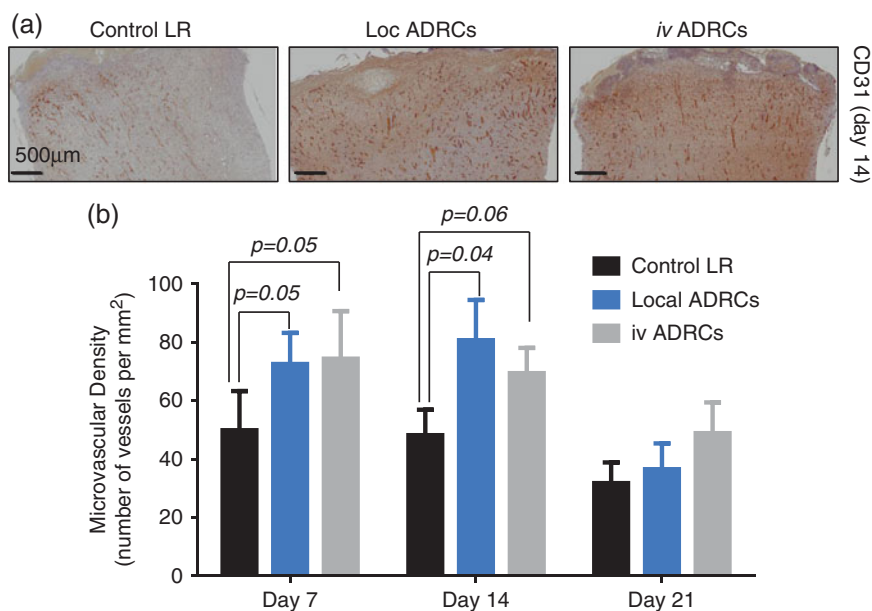


Figure 5. Effect of ADRC on wound vascularization after concomitant radiation and burn injury. (a) Skin biopsies collected from animals receiving LR or ADRC (local or iv) were stained for CD31. Representative photomicrographs of sections stained with CD31 at day 14 are shown. (b) Microvessel density (MVD) was quantified using automated analysis of digitally scanned slides. $n = 4-6$ animals/group ($n = 24-36$ wounds per group). Results are presented as mean \pm standard error of mean (SEM).

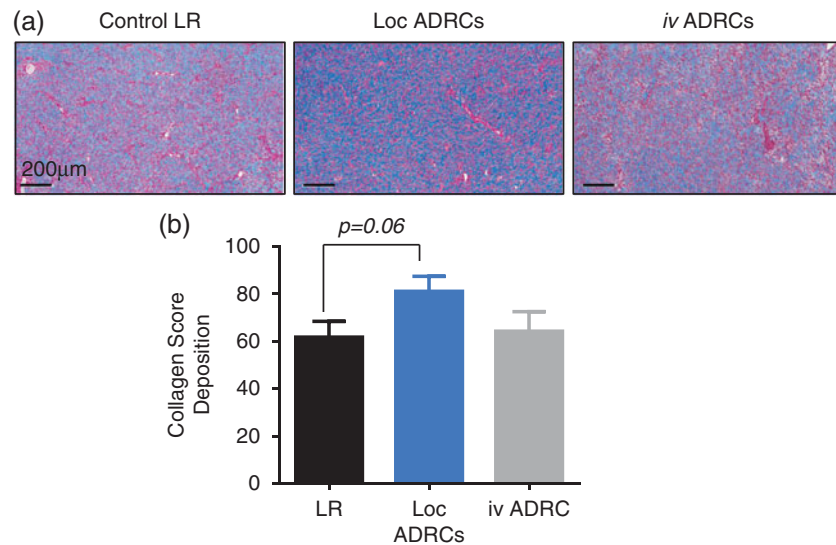


Figure 6. Effect of ADRC on collagen deposition after concomitant radiation and burn injury. (a) Skin biopsies collected from animals receiving LR or ADRC (local or iv) were stained for Masson Trichrome (MTC). Representative photomicrographs of sections stained with MTC at day 30 are shown. (b) Collagen deposition was quantified using automated positive pixel analysis of digitally scanned slides. $n = 4-6$ animals/group ($n = 24-36$ wounds per group). Results are presented as mean \pm standard error of mean (SEM).

reflecting the clinical situation of patients exposed to both thermal and radiation injury who are likely to be triaged to receive care following detonation of an improvised nuclear device. Despite an anticipated degree of inter-animal variability (unpublished data, LEBRI) the radiation dose applied in this model was sufficient to induce clinically significant damage to the hematologic system with neutrophil and platelet nadirs that approach and, in some animals exceed, those used as triggers for initiation of hematopoietic support (platelet transfusion and use of hematopoietic growth factors). Radiation related-toxicity was graded according to the system recommended by the Strategic National Stockpile Radiation Working Group (Waselenko et al. 2004). The hematopoietic toxicity achieved in this study corresponded to Grade 3 whereas cutaneous, neurovascular and gastrointestinal damage above Grade 1 was not observed in any of the animals enrolled.

The combination of this hematopoietic injury and the full thickness thermal burn injury was not lethal. In this way, the model accurately reflects the setting of a patient likely to be triaged to receive definitive burn care following a mass casualty event. Moreover, we have developed standardized procedures to induce reproducible full thickness burns and assess wound healing in irradiated animals. Our design was influenced by other published burn models describing wound excision after burn injury, skin grafting and wound assessment by planimetry (Branski et al. 2008; Singer et al. 2011; Foubert et al. 2015). Therefore, the knowledge obtained with the referred model may accelerate the assessment of new medical countermeasures to be deployed following a mass-casualty event involving detonation of an Improvised Nuclear Device (IND).

Current standard of care for burn injuries involves surgical excision and debridement of necrotic tissue and eschar followed by the application of autologous skin grafts or temporizing allograft, xenograft or tissue engineered skin substitutes. In a mass casualty event, it is likely that

availability of such therapies and modalities will be severely limited and that simpler therapeutic approaches will be preferred. Autologous cell therapy represents a novel strategy not only to address these challenges but also to promote wound healing and tissue repair. Uncultured ADRC/SVF cells have become an attractive source for regenerative medicine due to the relative ease of access and the abundance of regenerative cells within the mixed population (Fraser et al. 2006, 2014; Foubert et al. 2015). The use of an autologous cell therapy in the context of total body irradiation requires demonstration of the effectiveness of cells obtained from an irradiated individual to improve healing in that individual. It has been reported that high dose ionizing radiation (7–10 Gy) induces an acute response in mouse subcutaneous adipose tissue (Pogliano et al. 2009). The effects of lower doses on adipose tissue have not been reported. In the present study, our data demonstrate that viable, functional ADRC can be obtained from animals exposed to total body irradiation at a dose sufficient to induce significant damage to the hematopoietic system. Furthermore, these cells were capable of promoting wound vascularization, epithelialization and collagen deposition in the irradiated animals. The precise mechanism by which ADRC mediates this effect was beyond the scope of the present study. However, by extrapolation with data in other injury models it is likely mediated by paracrine release of factors by ADRC including vascular endothelial growth factor (VEGF), placental growth factor (PIGF), basic fibroblast growth factor (bFGF), and others (Feng et al. 2010; Kapur and Katz 2013; Kokai et al. 2014).

Re-epithelialization is the major clinical parameter assessed by both macroscopic and microscopic approaches in human as well as in preclinical wound of during burn wound healing. Treatment with ADRC administered either locally or systemically improved epithelialization in these study groups.

Vascularization of the wound bed is critical for healing (Gurtner et al. 2008). In our study, both locally and

intravenously injected ADRC increased blood vessel density within the wound site after combined radiation and burn injury. These findings are consistent with the recent demonstration of ADRC-mediated increased vascularity of excised porcine thermal burns treated with a widely-used skin substitute (Foubert et al. 2015) and with several studies demonstrating ADRC/SVF-induced angiogenesis in both acute and chronic injury models (Ebrahimian et al. 2009; Kondo et al. 2009; Akita et al. 2012; Atalay et al. 2014; Hao et al. 2014). There are also several small clinical case series and case reports demonstrating healing of previously refractory wounds following treatment with ADRC (Cervelli et al. 2011; Akita et al. 2012; Marino et al. 2013). These studies include healing in patients with chronic wounds resulting from radiotherapy for malignant disease (Akita et al. 2012).

While questions regarding optimal route of administration and specific mechanism of action remain to be answered, ADRC therapy represents a promising strategy to promote cutaneous repair after combined radiation and thermal burn injury.

It is important to note that the model described herein has several limitations and further investigations are required to improve it. First, the goal was to develop a model and to execute a pilot study demonstrating the capacity of the model to evaluate an autologous cell therapy. As such it included relatively small burn wounds, a single radiation dose and a single dose of ADRC. The radiation dose and burn size applied herein were selected to reflect the level of injury and prodromal symptoms that might be present in a patient triaged to receive care following a mass casualty event. In a mass casualty scenario, the logistic reality would likely preclude the allocation of scarce resources for large burns and/or higher radiation dose exposure. This study reflects this consideration. Therefore, future studies are required to assess lethality of more severe combined injury by expanding the model to burns of 10–20% total body surface area (or greater) and to higher doses of radiation. Each of these changes can be expected to have considerable impact on hematopoietic aplasia and healing. Assessment of parameters related to scarring and fibrosis or to other effects of radiation at much later time points (e.g. 6 and 12 months' post-treatment) will be interesting. However, long duration, large animal studies are extremely expensive. The current study was designed to develop a model whereby these and other parameters could be assessed in more detail. Planning for longer term studies is underway.

In conclusion, the model presented herein describes for the first time standardized procedures to create a reproducible minipig model of thermal burn injury complicated by concomitant radiation exposure that can be used to evaluate potential therapeutic countermeasures. Use of this model with a particular candidate countermeasure, autologous ADRC, demonstrated that this approach has the potential to promote wound re-epithelialization and vascularity in this context.

Disclosure statement

PF, AG, ZA, SZ and JKF are paid employees and stock holders of Cytori Therapeutics, Inc., San Diego. MT receives consulting fees from Cytori

Therapeutics, Inc. DZ, MDE, FB and WW have no conflicts of interest with regard to this study. The authors alone are responsible for the content and writing of the paper.

Funding

This work was supported by contract HHSO100201200008C from the Biomedical Advanced Research and Development Authority (BARDA), Department of Health and Human Services. DZ was supported by a grant from the California Institute for Regenerative Medicine (CIRM; TB1-01175).

References

- Akita S, Yoshimoto H, Ohtsuru A, Hirano A, Yamashita S. 2012. Autologous adipose-derived regenerative cells are effective for chronic intractable radiation injuries. *Radiat Prot Dosimetry*. 151:656–660.
- Atalay S, Coruh A, Deniz K. 2014. Stromal vascular fraction improves deep partial thickness burn wound healing. *Burns*. 40:1375–1383.
- Barabanova AV. 2006. Significance of beta-radiation skin burns in Chernobyl patients for the theory and practice of radiopathology. *Vojnosanit Pregl*. 63:477–480.
- Branski LK, Mittermayr R, Herndon DN, Norbury WB, Masters OE, Hofmann M, Traber DL, Redl H, Jeschke MG. 2008. A porcine model of full-thickness burn, excision and skin autografting. *Burns*. 34:1119–1127.
- Cervelli V, Gentile P, De AB, Calabrese C, Di SA, Scioli MG, Curcio BC, Felici M, Orlandi A. 2011. Application of enhanced stromal vascular fraction and fat grafting mixed with PRP in post-traumatic lower extremity ulcers. *Stem Cell Res*. 6:103–111.
- Colby C, Chang Q, Fuchimoto Y, Ferrara V, Murphy M, Sackstein R, Spitzer TR, White-Scharf ME, Sachs DH. 2000. Cytokine-mobilized peripheral blood progenitor cells for allogeneic reconstitution of miniature swine. *Transplantation*. 69:135–140.
- Cuttle L, Kempf M, Phillips GE, Mill J, Hayes MT, Fraser JF, Wang XQ, Kimble RM. 2006. A porcine deep dermal partial thickness burn model with hypertrophic scarring. *Burns*. 32:806–820.
- Ebrahimian TG, Pouzoulet F, Squiban C, Buard V, Andre M, Cousin B, Gourmelon P, Benderitter M, Casteilla L, Tamarat R. 2009. Cell therapy based on adipose tissue-derived stromal cells promotes physiological and pathological wound healing. *Arterioscler Thromb Vasc Biol*. 29:503–510.
- Feng Z, Ting J, Alfonso Z, Strem BM, Fraser JK, Rutenberg J, Kuo HC, Pinkernell K. 2010. Fresh and cryopreserved, uncultured adipose tissue-derived stem and regenerative cells ameliorate ischemia-reperfusion-induced acute kidney injury. *Nephrol Dial Transplant*. 25:3874–3884.
- Forcheron F, Agay D, Scherthan H, Riccobono D, Herodin F, Meineke V, Drouet M. 2012. Autologous adipocyte derived stem cells favour healing in a minipig model of cutaneous radiation syndrome. *PLoS One*. 7:e31694.
- Foubert P, Barillas S, Gonzalez AD, Alfonso Z, Zhao S, Hakim I, Meschter C, Tenenhaus M, Fraser JK. 2015. Uncultured adipose-derived regenerative cells (ADRCs) seeded in collagen scaffold improves dermal regeneration, enhancing early vascularization and structural organization following thermal burns. *Burns*. 41:1504–1516.
- Fraser JK, Hicok KC, Shanahan R, Zhu M, Miller S, Arm DM. 2014. The celution system: automated processing of adipose-derived regenerative cells in a functionally closed system. *Adv Wound Care (New Rochelle)*. 3:38–45.
- Fraser JK, Wulur I, Alfonso Z, Hedrick MH. 2006. Fat tissue: an underappreciated source of stem cells for biotechnology. *Trends Biotechnol*. 24:150–154.
- Gardien KL, Middelkoop E, Ulrich MM. 2014. Progress towards cell-based burn wound treatments. *Regen Med*. 9:201–218.
- Gurtner GC, Werner S, Barrandon Y, Longaker MT. 2008. Wound repair and regeneration. *Nature*. 453:314–321.
- Hao C, Shintani S, Shimizu Y, Kondo K, Ishii M, Wu H, Murohara T. 2014. Therapeutic angiogenesis by autologous adipose-derived regenerative

- cells: comparison with bone marrow mononuclear cells. *Am J Physiol Heart Circ Physiol.* 307:H869–H879.
- Huang SP, Huang CH, Shyu JF, Lee HS, Chen SG, Chan JY, Huang SM. 2013. Promotion of wound healing using adipose-derived stem cells in radiation ulcer of a rat model. *J Biomed Sci.* 20:51.
- Iijima S. 1982. Pathology of atomic bomb casualties. *Acta Pathol Jpn.* 32 Suppl 2:237–270.
- Kapur SK, Katz AJ. 2013. Review of the adipose derived stem cell secretome. *Biochimie.* 95:2222–2228.
- Kiang JG, Ledney GD. 2013. Skin injuries reduce survival and modulate corticosterone, C-reactive protein, complement component 3, IgM, and prostaglandin E 2 after whole-body reactor-produced mixed field (n + gamma-photons) irradiation. *Oxid Med Cell Longev.* 2013:821541.
- Kiang JG, Zhai M, Liao PJ, Elliott TB, Gorbunov NV. 2014. Ghrelin therapy improves survival after whole-body ionizing irradiation or combined with burn or wound: amelioration of leukocytopenia, thrombocytopenia, splenomegaly, and bone marrow injury. *Oxid Med Cell Longev.* 2014:215858.
- Kokai LE, Marra K, Rubin JP. 2014. Adipose stem cells: biology and clinical applications for tissue repair and regeneration. *Transl Res.* 163:399–408.
- Kondo K, Shintani S, Shibata R, Murakami H, Murakami R, Imaizumi M, Kitagawa Y, Murohara T. 2009. Implantation of adipose-derived regenerative cells enhances ischemia-induced angiogenesis. *Arterioscler Thromb Vasc Biol.* 29:61–66.
- Marino G, Moraci M, Armenia E, Orabona C, Sergio R, De SG, Capuozzo V, Barbarisi M, Rosso F, Giordano G, et al. 2013. Therapy with autologous adipose-derived regenerative cells for the care of chronic ulcer of lower limbs in patients with peripheral arterial disease. *J Surg Res.* 185:36–44.
- Moroni M, Ngudiankama BF, Christensen C, Olsen CH, Owens R, Lombardini ED, Holt RK, Whitnall MH. 2013. The Gottingen minipig is a model of the hematopoietic acute radiation syndrome: G-colony stimulating factor stimulates hematopoiesis and enhances survival from lethal total-body gamma-irradiation. *Int J Radiat Oncol Biol Phys.* 86:986–992.
- Palmer JL, Deburghgraeve CR, Bird MD, Hauer-Jensen M, Kovacs EJ. 2011. Development of a combined radiation and burn injury model. *J Burn Care Res.* 32:317–323.
- Pennington LR, Sakamoto K, Popitz-Bergez FA, Pescovitz MD, McDonough MA, Macvittie TJ, Gress RE, Sachs DH. 1988. Bone marrow transplantation in miniature swine. I. Development of the model. *Transplantation.* 45:21–26.
- Poglio S, Galvani S, Bour S, Andre M, Prunet-Marcassus B, Penicaud L, Casteilla L, Cousin B. 2009. Adipose tissue sensitivity to radiation exposure. *Am J Pathol.* 174:44–53.
- Riccobono D, Agay D, Scherthan H, Forcheron F, Vivier M, Ballester B, Meineke V, Drouet M. 2012. Application of adipocyte-derived stem cells in treatment of cutaneous radiation syndrome. *Health Phys.* 103:120–126.
- Singer AJ, Hirth D, McClain SA, Crawford L, Lin F, Clark RA. 2011. Validation of a vertical progression porcine burn model. *J Burn Care Res.* 32:638–646.
- Singer AJ, McClain SA. 2003. A porcine burn model. *Methods Mol Med.* 78:107–119.
- Sullivan TP, Eaglstein WH, Davis SC, Mertz P. 2001. The pig as a model for human wound healing. *Wound Repair Regen.* 9:66–76.
- United States Government Accountability Office. 2012. National Preparedness: Countermeasures for Thermal Burns. *Bibliogov.*
- Valente M, Denis J, Grenier N, Arvers P, Foucher B, Desangles F, Martigne P, Chaussard H, Drouet M, Abend M, et al. 2015. Revisiting biomarkers of total-body and partial-body exposure in a baboon model of irradiation. *PLoS One.* 10:e0132194.
- Waselenko JK, Macvittie TJ, Blakely WF, Pesik N, Wiley AL, Dickerson WE, Tsu H, Confer DL, Coleman CN, Seed T, et al. 2004. Medical management of the acute radiation syndrome: recommendations of the Strategic National Stockpile Radiation Working Group. *Ann Intern Med.* 140:1037–1051.
- Williams JP, Brown SL, Georges GE, Hauer-Jensen M, Hill RP, Huser AK, Kirsch DG, Macvittie TJ, Mason KA, Medhora MM, et al. 2010. Animal models for medical countermeasures to radiation exposure. *Radiat Res.* 173:557–578.